THE JOURNAL OF PHYSICAL CHEMISTRY B

Article

pubs.acs.org/JPCB

DNA Origami Metallized Site Specifically to Form Electrically Conductive Nanowires

Anthony C. Pearson,[†] Jianfei Liu,[‡] Elisabeth Pound,[§] Bibek Uprety,[‡] Adam T. Woolley,*[,§] Robert C. Davis,*[,†] and John N. Harb*[,‡]

[†]Department of Physics and Astronomy, [‡]Department of Chemical Engineering, and [§]Department of Chemistry and Biochemistry, Brigham Young University, Provo, Utah 84602, United States

Supporting Information

ABSTRACT: DNA origami is a promising tool for use as a template in the design and fabrication of nanoscale structures. The ability to engineer selected staple strands on a DNA origami structure provides a high density of addressable locations across the structure. Here we report a method using site-specific attachment of gold nanoparticles to modified staple strands and subsequent metallization to fabricate conductive wires from DNA origami templates. We have modified DNA origami structures by lengthening each staple strand in select regions with a 10-base nucleotide sequence and have attached DNA-modified gold nanoparticles to the lengthened staple strands via complementary base-pairing. The high density of extended staple strands allowed the gold nanoparticles to pack tightly in the modified regions of the DNA origami, where the measured median gap size between neighboring particles was 4.1 nm. Gold metallization processes were optimized so that the attached gold nanoparticles grew until gaps between particles were filled and uniform continuous nanowires were formed. Finally, electron beam lithography was used to pattern electrodes in order to measure the electrical conductivity of metallized DNA origami, which showed an average resistance of 2.4 kΩ per metallized structure.

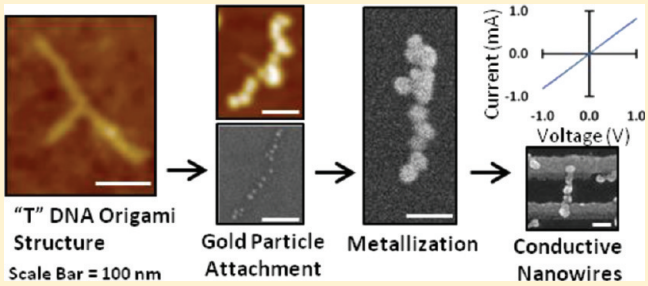

Self-assembly methods have shown promise for the fabrication of complex structures with extremely small feature sizes.[1,2] Scaffolded DNA origami, in particular, provides a robust and simple method for designing patterned shapes in the sub-100-nm regime. The DNA origami technique can produce a wide variety of two-dimensional,[3,4] as well as three-dimensional,[5−9] structures by folding a long, single-stranded DNA "scaffold" into a designed shape with use of a large number of shorter "staple" strands consisting of synthetic DNA. A distinct advantage of DNA origami is that the staple strands can be adjusted to engineer site-specific attachment points throughout the structure. Location-selective variability can be achieved either by direct chemical modification at the ends of staple strands or by extending staple strands with additional nucleotides and hybridizing these "sticky ends" with a complementary sequence containing the desired functional group or moiety. Using these techniques, a variety of materials have been controllably attached to DNA origami such as RNA probes,[10] proteins,[11−14] carbon nanotubes,[15] and metallic nanoparticles.[16−21]

The use of DNA origami structures as templates for metallization is potentially enabling for technologies such as nanoelectronic circuits[22] and plasmonics,[23,24] among others. Although there is a considerable body of literature describing the metallization of linear, double-stranded DNA,[25−28] we were the first to report the continuous metallization of DNA origami,[29] which was followed by a few more recent reports.[30−32] One particularly attractive aspect of molecularly templated nanofabrication is the possibility of dictating the precise location of metallization. Site-specific metallization is possible with DNA origami where the recognition properties of DNA can be used to create the complex structures needed, for example, for nanocircuit formation. Also, for many applications, it is imperative that the metallized structures are continuous and conductive. While much work has been done previously to characterize the conductivity of nanowires templated by linear DNA, this study is, to our knowledge, the first to verify continuity and conductivity of nanowires templated by DNA origami. This is due to difficulties in both fabrication and measurement. Fabrication of conductive nanowires on a DNA origami template is complicated due to the difficulty of achieving high seed density, plating precision, and high stability of the DNA origami during the plating process.[29] Site-specific placement of seeds causes limitations in seed density, since the spacing between available attachment points is controlled by the staple strand spacing. Additionally, the seeds must be

Special Issue: Richard A. Mathies Festschrift

Received: March 9, 2012
Revised: April 24, 2012
Published: April 26, 2012

   dx.doi.org/10.1021/jp302316p | J. Phys. Chem. B 2012, 116, 10551−10560

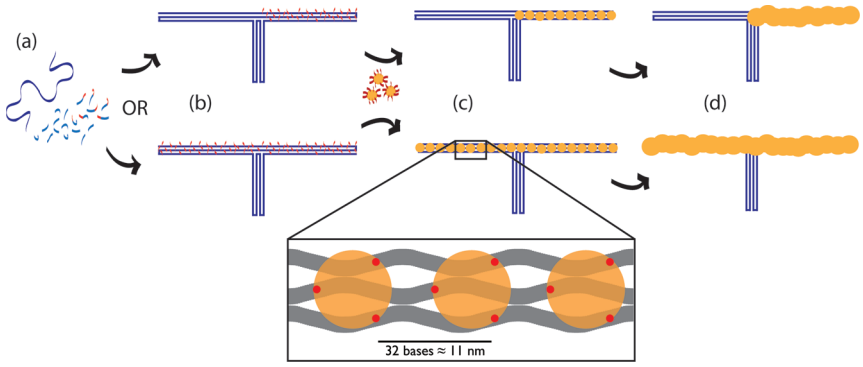

Figure 1. Process used for site-specific seeding by attachment of Au NPs and subsequent metallization. (a) Regular (blue) and modified (red portion) staple strands are used to fold a branched "T" DNA origami structure. (b) The location of modified staple strands is programmed based on desired regions for particle attachment. (c) Au NPs coated with DNA complementary to the modified staples are added and attached to the DNA structure. A section is enlarged to show spacing of attached Au NPs along the DNA structure. (d) A subsequent metallization procedure grows the particles until a continuous metal wire is formed across the locations seeded by Au NPs.

chemically modified prior to attachment and metallization, which may affect the metallization process. The focus of the present study is on the fabrication and characterization of conductive nanowires by site-specific metallization of origami templates.

Recently, site-specific metallization of a modular, 100 nm × 100 nm DNA origami tile was reported by Pais et al.[31] In that report, metal structures of a few different shapes were formed by electroless plating of silver onto gold nanoparticles placed at specific sites on the DNA origami tiles. Our work provides at least three distinct advances toward enabling functional electronic device fabrication using site-specific metallization of DNA origami: (1) our metallization process was developed to create conductive nanowires needed for devices and includes experimental verification of conductivity; (2) our thin, branched DNA origami structures which we have previously reported[29,30,33] allow for considerably longer wires than is possible with a modular and dense tile motif; (3) the high seed density achieved herein permits the fabrication of continuous nanowires of very small diameter.

RESULTS AND DISCUSSION

Figure 1 demonstrates the assembly process for our site-specific metallization of DNA origami structures to form metallic nanowires. The DNA origami structure shown is a branched "T" structure, which was formed as previously reported[33] except where staple strands are extended by an A_{10} sequence on the 3′ end in selected locations (Figure 1a,b). After folding the DNA origami, excess staples were removed by filtering. Gold nanoparticles (Au NPs) nominally 5 nm in diameter were conjugated with thiolated T_8 DNA according to an established protocol[16,34] and combined with the DNA origami (Figure 1b,c). Attachment of the T_8 DNA-linked Au NPs to the extended A_{10} staple strands on the DNA origami creates "seeds" along specific sections of the DNA structure for further metal deposition (Figure 1c,d).

The attachment sites, or A_{10} extensions, on the DNA origami were positioned on every staple strand within the desired sections, making them about 11 nm apart along each double helix and in a staggered pattern with adjacent helices (see red dots in zoomed in region of Figure 1c). Since multiple thiolated DNA strands are attached to each Au NP and each staple strand extension on the DNA origami contains the same DNA attachment sequence, a 5 nm Au NP could bind easily to the DNA origami through as many as three (and perhaps four) of the extended staple strands. In initial Au NP seeding experiments, "T" origami structures were designed to have Au NPs bind to only one-half of the top section of the DNA origami (see upper structure in Figure 1b). This portion is ∼120 nm long and contains 33 positions for approximately 11 Au NPs to attach.

When Au NPs were mixed in solution with the DNA origami at a ratio of about 12:1 Au NPs to DNA origami, the section with Au NPs attached almost always appeared significantly shorter by atomic force microscopy (AFM) than before Au NP seeding. To explore this phenomenon, ratios of Au NPs to DNA origami of about 1:1, 19:1, and 27:1 were also tested. The 1:1 ratio samples looked very similar to the seeded samples with a 12:1 ratio. In both samples, instead of a Au NP (or a few Au NPs) spread somewhere along the portion of the "T" which contained attachment points, the modified section generally looked truncated with the Au NPs near the junction of the "T" structure (see the Supporting Information for AFM images). Increasing the ratio of Au NPs mixed with DNA origami to ∼19:1 yielded some longer seeded segments, and increasing the ratio to ∼27:1 gave even more seeded segments close to the unseeded length (see Figure 2a and the Supporting Information). It is possible that when an insufficient number of Au NPs are available for attachment the DNA origami can wrap or fold around attached Au NPs, causing it to appear shorter. Occasionally, in samples with the highest Au NP to origami ratio, there are what appear to be origami aggregates. It is possible that in some of these instances Au NPs are binding and connecting two origami structures together. However, since origami were also seen lying very close together in some samples of unseeded origami, it is difficult to quantify this effect.

To increase the length of the seeded region, the DNA origami design was modified so the staple strands were extended across the entire top section of the "T" structure (see bottom structure in Figure 1b). This section is ∼240 nm long and contains 67 total extended staple strands for approximately 22 Au NPs to attach. When Au NPs were attached in solution to this structure, the two sides of the top section usually folded together with some Au NPs attached to both sides (see Figure 2b). Since the entire top section contains the same attachment sequence and the "T" structure is somewhat flexible, this was a reasonable, but undesired, result.

dx.doi.org/10.1021/jp302316p | J. Phys. Chem. B 2012, 116, 10551−10560

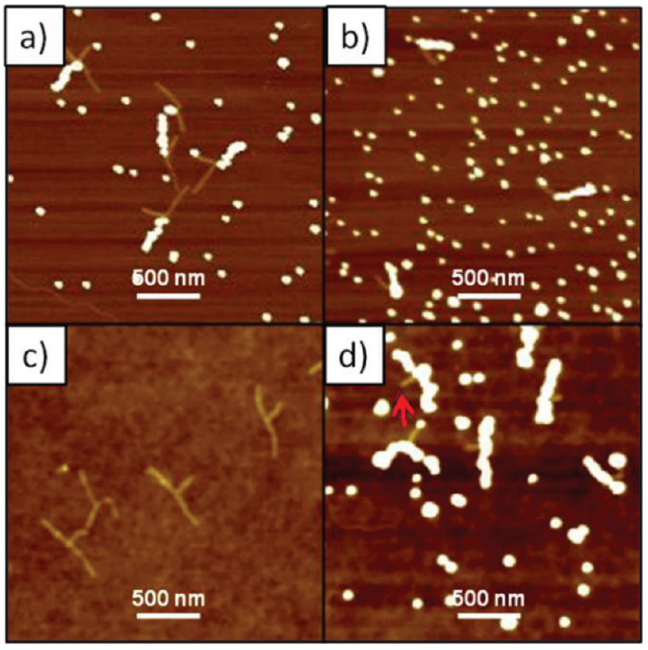

Figure 2. Tapping mode AFM images of "T" DNA origami structures. (a) "T" DNA origami with modified staple strands along half of the top section after the Au NP attachment process was done in solution. Here a ratio of ~27:1 Au NPs to DNA origami was used. (b) "T" DNA origami with modified staple strands along the entire top section after the Au NP attachment process. For parts a and b, samples were deposited on mica surfaces for imaging. (c) Unseeded "T" DNA origami deposited on a SiO_2 surface. (d) "T" DNA origami seeded with Au NPs after surface deposition on SiO_2. The red arrow points to the unseeded portion on the origami. The height scale in all images is 6 nm.

The problem of simultaneous attachment may be addressed in multiple ways, for instance, by using staple strands with different binding sequences on each arm. In this study, we resolved the matter by depositing DNA origami first on a thermally grown silicon dioxide surface and then exposing the surface to the Au NP solution to permit gold particles to interact with the deposited DNA origami.

To achieve stable adsorption of the DNA origami on the oxide surface, we followed the process reported by Kershner et al.[35] Specifically, a solution of DNA origami (0.67 nM), containing sticky ends modified as shown in the bottom design of Figure 1b, was left on the surface for 2 h to allow magnesium ions to bind the negatively charged DNA structures to a plasma cleaned, negatively charged silicon dioxide surface.

Figure 2c shows an AFM image of "T" DNA origami on a SiO_2 surface prior to seeding with Au NPs, and Figure 2d shows the DNA origami following Au NP attachment. It is clear that the particles have attached to the top portion of the "T" origami as intended, since the region not modified for Au NP attachment (marked with an arrow in Figure 2d) is clearly seen. Comparison of Figure 2c and d shows that the shape of the "T" origami is well conserved during the Au NP attachment process, since the top portion has consistent curvature and length before and after attachment. The purpose of the attachment of Au NPs is to create sites on the origami which can be further metallized to form a conductive segment or nanowire. In order to obtain nanowires with the smallest possible dimensions, it is essential to have Au NPs spaced as closely as possible in the desired region on the origami. Since AFM imaging cannot resolve spacing between particles because of tip effects (Figure 3a), scanning electron microscopy (SEM)

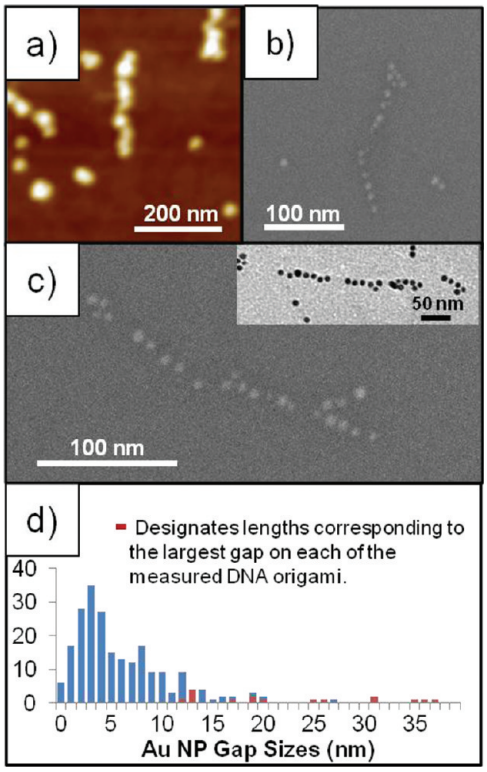

Figure 3. (a) Tapping mode AFM image of Au NP seeded DNA origami (zoomed and adjusted height scale from Figure 2d; height scale 20 nm). (b, c) Examples of high resolution SEM images used to determine the center-to-center spacing of Au NPs seeded on DNA origami. The inset in part c shows a bright field TEM image of a Au NP seeded DNA origami. (d) Histogram of the gap sizes between particles on the seeded DNA origami. The red bars correspond to the largest gap size in each of the measured DNA origami.

and transmission electron microscopy (TEM) were used to examine particle location and spacing, and to provide quantitative measurements of the size of gaps between Au NPs.

SEM samples were prepared using surface seeding of "T" DNA origami on thermally grown SiO_2 surfaces as explained above, and TEM samples were prepared by surface deposition and seeding of the DNA origami on a 40 nm silicon monoxide film supported on a copper TEM grid. SEM data (Figure 3b,c) shows the average length of the seeded portion of the DNA origami to be 195 nm. On average, there were 16 Au NPs attached to each DNA origami, and the median center-to-center spacing was 11.7 nm. A mean Au NP diameter of 7.6 nm, found by measuring particle sizes from high resolution TEM images, was used to estimate the corresponding gap size between particles (see inset of Figure 3c). Thus, we estimate the median gap between Au NPs to be 4.1 nm. However, often in one or more locations, there were larger gaps between Au NPs (see Figure 3d).

Interestingly, our microscopy analysis has shown that the Au NPs generally line up in single file along the DNA origami with a median center-to-center spacing (11.7 nm) that nearly matches the sticky end spacing on each of the three double helices on the top portion of the "T" origami (10.5−11 nm). This likely means that the Au NPs are attaching to sets of three sticky ends, as indicated in the zoomed region of Figure 1c.

dx.doi.org/10.1021/jp302316p | J. Phys. Chem. B 2012, 116, 10551−10560

When all Au NPs attached to the DNA origami are considered, the ratio of total extended staple strands to Au NPs is 4.19. However, when only the regions with no large gaps between Au NPs are considered, the ratio becomes 2.75. We can conclude that the Au NPs are generally attached to three sticky ends, although some attachment of Au NPs to only two sticky ends also must occur.

These results show closer Au NP spacing than previously reported techniques. This may be due to the use of a short T_8 strand to link the Au NPs to the DNA origami. Because of the short persistence length of single-stranded DNA, the length of the T_8 strand is ~2 nm in solution.[36] Thus, the effective diameter of the particle is ~11.6 nm, similar to our median center-to-center spacing. Additionally, the high density of available binding locations that we have used increases the probability that a Au NP will attach when it interacts with the DNA origami, making it more likely that particles will attach with the minimum possible spacing.

Following seeding, our goal was to selectively plate the Au NP seeds with gold until continuous wires formed. The minimum possible wire width following the plating step is limited by the largest gap between Au NPs. To fill a gap with a plating process, the width of the Au NP seeds must increase by at least the gap size, or equivalently, the radius of each seed must increase by at least half of the gap size. From Figure 3d, we see that our maximum gap sizes on each DNA origami ranged from 12 to 37 nm (median value was 19 nm). Assuming hemispherical growth of the seeds, we expect that most wires 26.6 nm (7.6 nm Au NP width + 19 nm gap size) or larger in width would be continuous across the length of the seeded portion of the branched origami. However, continuous wires of 11.7 nm in width could be achieved if all gaps between Au NPs equaled the median gap size (7.6 nm Au NP width + 4.1 nm median gap size). Adjustment of seeding parameters such as Au NP size, Au NP:origami ratio, oligonucleotide linker length, and seeding temperature and time will help to achieve this result.

To selectively plate the Au NP seeds, we used a modified commercial Au plating solution to which 10 mM $MgCl_2$ was added (see Materials and Methods below). Figure 4a–h shows SEM results for samples plated for 1, 2, 5, and 20 min. Figure 4i shows the width of DNA nanowires plated for 5, 10, and 20 min, since these times were long enough for many nanowires to appear continuous by SEM.

After 1 min of plating, the average width of the Au NPs on the DNA origami increased by 5.4 nm from the initial seeded width (7.6 nm). SEM imaging (Figure 4a,b) showed that the nanowires formed were not continuous at this stage. This is not surprising, since the amount of growth was not sufficient to fill in the larger gaps (≥12 nm) that occurred periodically between the seeds. After 2 min of plating, metallization appeared continuous for some of the origami, since the increase in the plated width was sufficient to span the "large" gaps that were on the order of 12 or 13 nm (Figure 4c,d; see also histogram in Figure 3d). The general trend toward increased connectivity continued with the longer plating times (Figure 4); in addition, the plating rate decreased with plating time (5.4 nm/min after 1 min and 0.87 nm/min after 20 min) and the uniformity of the nanowires appeared to get worse as the plating time increased.

The substantial decrease in the plating rate with time indicates the potential importance of reactant transport. In fact, the observed rate of metal accumulation was close to that calculated by assuming that the plating process was diffusion

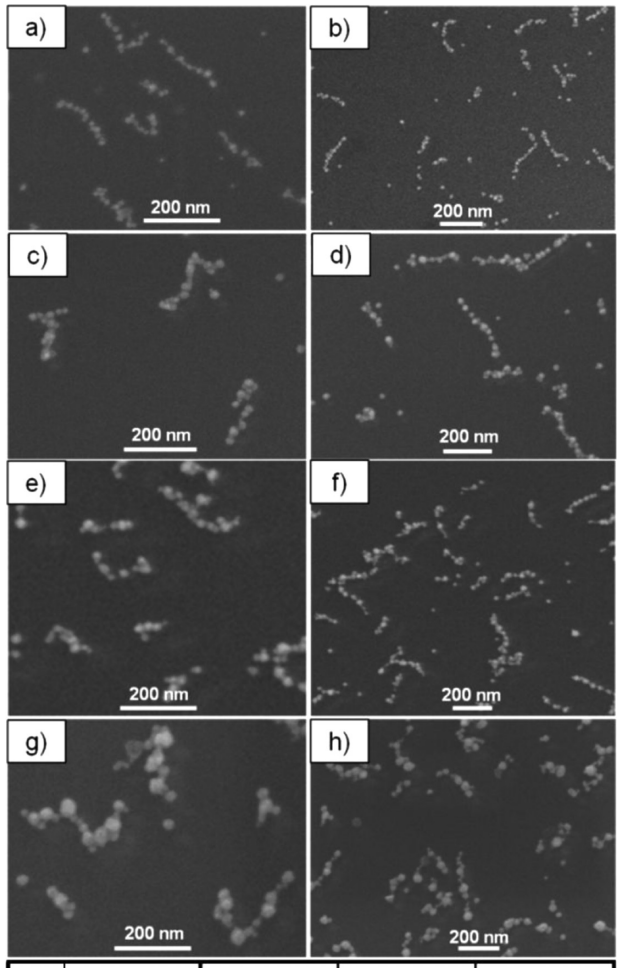

i) Time (min)	5	10	20
Nanowire Width (nm)	18.3 ± 6.1	19.8 ± 7.2	25.0 ± 11.4

Figure 4. SEM images following Au plating of the Au NP seeds on the "T" DNA origami with a modified commercial plating solution. (a, b) DNA origami plated for 1 min. (c, d) DNA origami plated for 2 min. (e, f) DNA origami plated for 5 min. (g, h) DNA origami plated for 20 min. (i) A table of the average widths (measured from SEM data) of the plated DNA origami for the plating times indicated.

limited. To further explore the role of mass transfer in the plating process, plating was done on a control surface with no DNA origami and sparse Au seeds, which were prepared and coated with DNA-thiol as discussed above. The sparse seed spacing (less than 15 Au seeds in an area of 10 μm by 10 μm) permitted a much higher rate of transport to the seeds. When plated for 2 min, the seeds grew to an average height of 49 nm, much taller than that on the surfaces with a high density of seeded DNA origami, and consistent with expectations.

The depletion of reactants during plating of the DNA origami implies that a higher plating rate might be achieved if multiple plating steps, each using a fresh plating solution, were done for each sample. When a surface containing seeded DNA origami was plated twice with fresh plating solution, each time for 3 min, the average width of the plated DNA origami was 35 ± 14 nm, significantly larger than samples plated for 20 min with one solution (Figure 5a,b). However, the width across individual wires varied substantially from 10 to 65 nm, causing

dx.doi.org/10.1021/jp302316p | J. Phys. Chem. B 2012, 116, 10551–10560

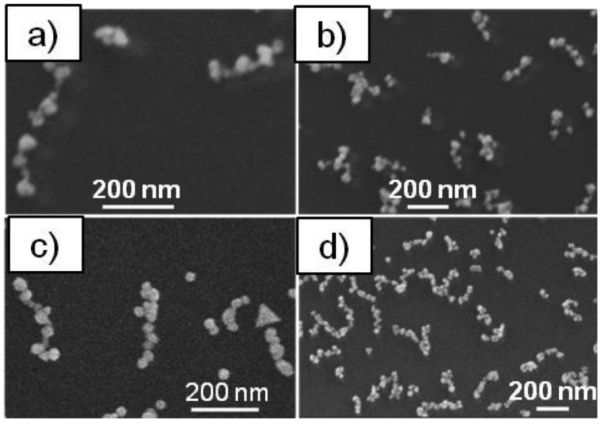

Figure 5. SEM images of plated "T" DNA origami. (a, b) DNA origami plated twice for 3 min each using the modified commercial plating solution (with Mg^{2+} added). (c, d) Origami plated with the modified commercial Au plating solution for 1 min and Natan's Au plating solution for 2 min.

the morphology of the nanowires to look similar to beads on a string, since some sections plated at a much higher rate than others. This is similar to the morphology seen in the sample plated once for 20 min shown in Figure 4g. While the plating rate was significantly increased by plating in two steps, the nanowires were still nonuniform, reflecting the possible limiting role of mass transport.

Because of limitations with the Au plating solution demonstrated above, that solution is unlikely to result in uniform deposition under the conditions of interest to this work. In contrast, Satti et al.[37] observed more uniform plating of gold on λ-DNA with a solution consisting of $HAuCl_4$ and NH_2OH that had been used earlier by Natan et al.[38] to enlarge Au NPs. This plating solution did not appear to work in our initial experiments, which showed no observable increase in the size of Au NPs exposed to the solution. Apparently, the functionalization of the Au NPs with oligonucleotides or perhaps residual citrate or BSPP inhibited plating. However, substantial plating was observed when DNA origami were plated for 1 min with the modified commercial solution and then plated for 2 min with the new solution (Natan's solution). The width of the metallized origami ranged from 19.4 to 38.9 nm with an average value of 33.0 nm and a standard deviation of 7.3 nm. This standard deviation is about half that observed for DNA origami plated to a similar width in multiple steps with the previous plating solution. Thus, the use of Natan's Au plating solution increased the uniformity of plating and yielded continuous structures, as shown in Figure 5c,d.

Electrical measurements were performed to determine the continuity of the DNA origami templated nanowires following metallization using Natan's plating solution. Sets of gold measurement electrodes were fabricated using electron beam lithography on SiO_2 surfaces which contained randomly oriented metallized DNA origami. The Au electrodes were formed by thermal evaporation of a 5 nm chromium adhesion layer followed by 40 nm of Au onto the lithographically patterned surface. The resist was removed by immersion in 1165 Microposit Remover at room temperature overnight. Each electrode set consisted of eight 50 μm × 50 μm Au pads (Figure 6a) connected to 100 nm wide measurement electrodes in parallel (see Figure 6b), with a gap between measurement electrodes of 160 nm. This geometry allowed measurement electrodes, which had been fabricated on top of the metallized origami, to make a connection across correctly oriented DNA origami. To measure the resistance between two electrodes, micromanipulator probes were placed on the corresponding 50 μm pads. The voltage between the electrodes was generally ramped from −100 to 100 mV, and up to 1.5 V was applied across some electrodes. The resulting electric current was measured with a picoammeter (Ithaco). As a control, electrode sets were fabricated on a SiO_2 substrate containing no metallized DNA origami, and voltages were applied across

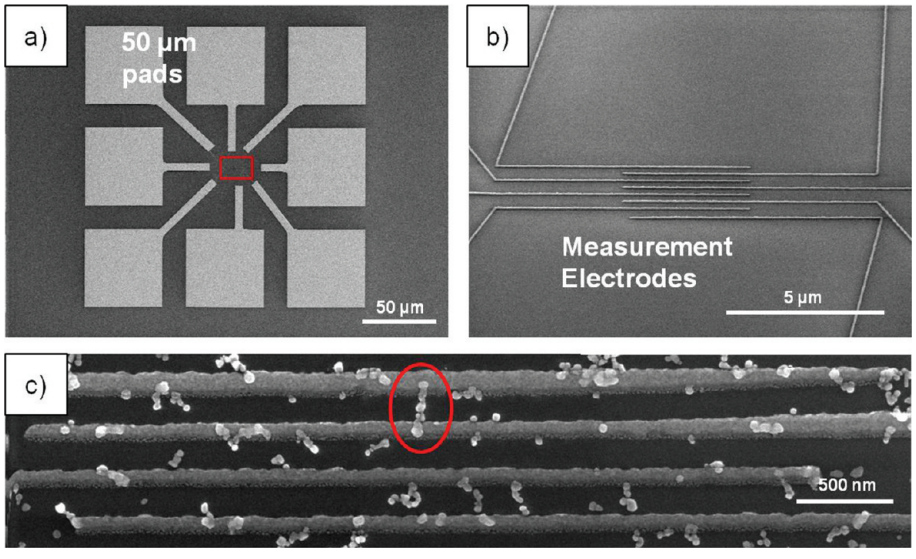

Figure 6. Electrode set geometry for electrical measurements of metallized DNA origami. (a) 50 μm pads allowing electrical connection by micromanipulator probes. (b) Zoom in of the region enclosed in the box in part a showing 100 nm electrodes running parallel. Parallel Au electrodes are 4 μm long with a gap of about 160 nm between electrodes. Image is on a sample containing no DNA origami. (c) Close-up of electrode set on a surface containing metallized DNA origami. Between the top two electrodes, marked with a red circle, is a single metallized DNA origami bridging the gap. Electrical measurements showed this origami to have a 2 kΩ resistance.

dx.doi.org/10.1021/jp302316p | J. Phys. Chem. B 2012, 116, 10551−10560

electrodes as in samples which contained metallized DNA origami.

To ensure that contact resistance between the micromanipulator probes and 50 μm Au pads did not substantially affect the measured resistances, two adjacent electrodes in a set of measurement electrodes were intentionally connected during the lithography step. Following the evaporation of chromium and gold and resist lift-off, the resistance across the connected measurement electrodes was 4 Ω, which we can assume is the maximum possible value of the contact resistance.

As voltages were applied across electrodes fabricated on a surface of metallized DNA origami, the number of electrically connected electrode pairs in a given electrode set was dependent on the local DNA origami surface concentration. In regions of high DNA origami surface concentration, electrode sets contained multiple locations where adjacent electrodes were connected by one or more metallized DNA origami. Electrode sets in DNA sparse regions often contained either zero or only one conductive origami bridging between electrodes, and electrical measurement of a control sample where electrode sets were fabricated on a SiO_2 surface containing no conductive origami did not show any adjacent electrodes which were electrically connected. Since the density of metallized DNA origami tended to decrease slightly during lithographic processing, a 2 nM solution of "T" DNA origami was used during initial deposition onto SiO_2 surfaces to achieve a surface density of metallized DNA origami sufficient for successful electrical measurements.

An example of a metallized DNA origami nanowire connecting between adjacent electrodes is circled in the upper middle of Figure 6c. The resistance between the top two electrodes in Figure 6c was 2.0 kΩ. The nanowire connecting the two electrodes measured 260 nm in length and 40 nm in width at the widest point. Figure 7a shows an example of an $I-V$ curve obtained during electrical probing. The linearity of the plot suggests that the DNA origami nanowires exhibit typical ohmic behavior up to 1 V. The breakdown current density was measured by ramping the voltage above 1 V. At 1.4 V, the current dropped to zero. Right before failure, the current density was 1.26×10^{12} A/m^2, which is similar to other breakdown current density measurements on DNA templated Au nanowires.[39]

The separation between the measured maximum and minimum resistances was approximately 1 kΩ, as shown in Figure 7b. Half of the measurements gave resistance values of ~1.5 kΩ. Upon SEM inspection, the resistance values scaled roughly with the number of DNA origami bridging the gap. The values between 1.75 and 2 kΩ correspond to electrode sets with one origami nanowire bridging between electrodes, while measurements below 1.75 kΩ generally came from electrode pairs with two origami nanowires bridging the gap. Electrodes with resistances near 1.5 kΩ generally were connected by two metallized DNA origami in which one (or both) had a region where the metallization was narrow (<15 nm). Due to narrow regions in the nanowires, the resistance across the electrodes was larger than electrodes connected by two uniformly metallized DNA origami (~1 kΩ) but still less than electrode pairs with a single uniformly metallized DNA origami (~2 kΩ). It was determined that on average the resistance per DNA origami was 2.3 kΩ with a standard deviation of 0.6 kΩ (18 total metallized DNA origami were measured). Using the average resistance and the average measured nanowire width of 33.0 nm, a resistivity value of 6.2×10^{-6} Ωm was calculated,

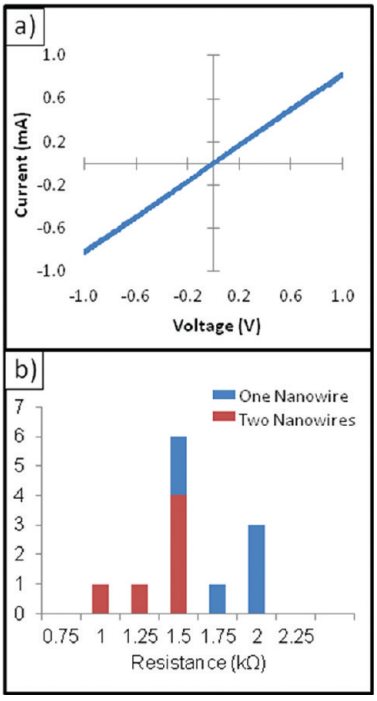

Figure 7. (a) Current−voltage plot of an electrode pair with resistance of 1.25 kΩ, where the voltage was ramped from −1 to 1 V. The device shows typical ohmic behavior over these voltages. (b) Histogram of 12 measured resistance values. SEM images show that devices with resistances less than 1.75 kΩ generally have two metallized DNA origami connecting between the two measurement electrodes.

which is in the same range as other reported values for both gold nanorods (3×10^{-6} Ωm)[40] and gold nanowires fabricated on linear double-stranded DNA (values range from 4×10^{-8} to 2×10^{-4} Ωm).[37,41] Our resistivity value is over 2 orders of magnitude higher than the bulk resistivity of gold (2.2×10^{-8} Ωm). Some resistivity increase can be expected from electron scattering from grain boundaries in the nanowires; additionally, poor connection between grains, defects, and impurities, possibly from the presence of nucleotides, could also contribute to the high resistivity. This is the first report showing the fabrication and electrical characterization of electrically conductive metallic structures templated by DNA origami. Thus, these results represent an important step toward enabling the use of DNA origami in the fabrication of functioning nanodevices.

Using DNA origami, we have demonstrated the ability to fabricate electrically conductive structures in a controlled geometry with feature sizes approaching the limitations of current industrial nanofabrication.[42] Such a technology can be useful in the fabrication of nanodevices for many applications. For example, in nanoelectronics, our technique could be used to fabricate separated source, drain, and gate electrodes for transistors. In order to create geometries useful for nanodevice fabrication, it is important to have the ability to design and control the location of separate metallized regions in the DNA origami structure. Here we demonstrate that this is possible using our "T" DNA origami. We have adjusted the design of the DNA origami so that the A_{10} extensions are only located on staple strands toward the ends of the top portion of the "T", as shown in Figure 8a. Seeding and metallization of this structure results in an ~100 nm gap between metallized portions. AFM or SEM images of the unseeded, seeded, and metallized

dx.doi.org/10.1021/jp302316p | J. Phys. Chem. B 2012, 116, 10551−10560

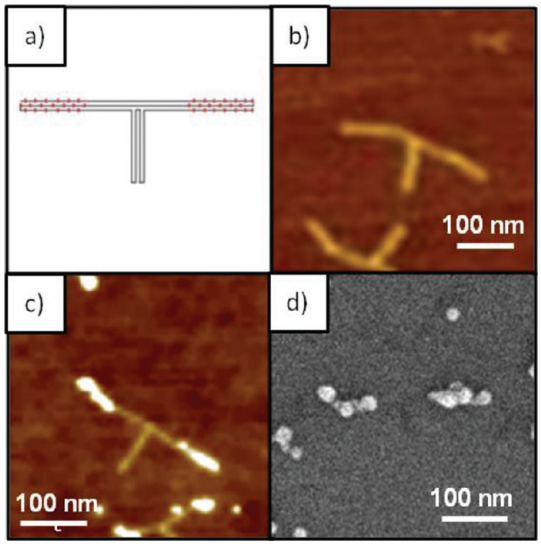

Figure 8. Images of the "T" shaped DNA origami with a programmed gap in which a semiconducting material could be deposited. (a) A schematic of the "T" structure where the red markings show the location of attachment. (b) Tapping mode AFM image of the unseeded "T" structure. The height scale is 4 nm. (c) Tapping mode AFM image of seeded "T" structure where a gap is seen between seeded regions. The height scale is 6 nm. (d) SEM image of the "T" DNA origami with a gap following metallization.

structure are shown in Figure 8b, c, and d, respectively. A geometry such as this could be used to form a transistor if a semiconducting material, such as a semiconducting carbon nanotube, were inserted between metallized regions.

We have also designed a DNA origami structure for site-specific metallization that can serve as a template for a simple logic device. Each staple strand of the structure was extended on the 3′ end with an A_{10} sequence with the exception of two gaps, as shown in Figure 9a. The Au NP seeding and metallization steps described for the "T" DNA origami were repeated for this structure. AFM images of the unseeded and seeded structure are shown in Figure 9b and c, respectively. As shown in Figure 9d, following metallization, structures have been formed and metallized correctly; however, in some cases, leads appear to have linked with a neighboring electrode due to partial over-metallization.

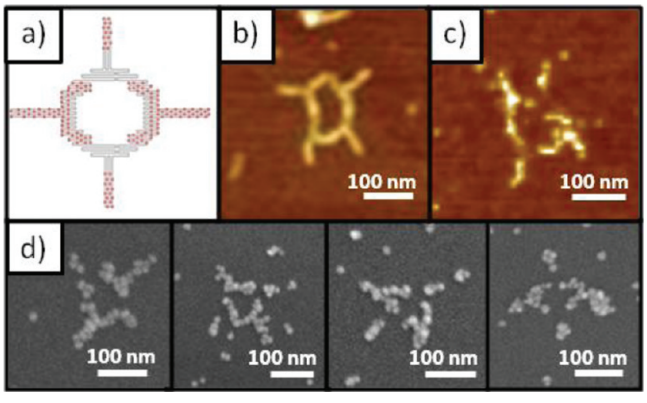

Figure 9. Logic gate prototype. (a) The structure of the DNA origami design, where the red markings show the location of staple strand A_{10} extensions for attachment. (b) Tapping mode AFM image of the DNA origami prior to seeding and metallization. The height scale is 4 nm. (c) Tapping mode AFM image of seeded DNA origami. The height scale is 16 nm. (d) SEM images of the prototype structure after the plating process.

Process optimization would enhance our ability to create large numbers of successful structures. Critical aspects of the fabrication process include the placement of the DNA origami templates on surfaces and selective site-specific metallization of these templates. While our yield of correctly folded origami is high (~70%), we find that fewer than 15% of the DNA origami deposit on the surface in an open geometry with the four leads directed outward, similar to the structures shown in Figure 9. The remaining DNA origami appear to have twisted, buckled, or aggregated on the surface during the deposition process, which limits the yield of potentially useful metallized structures after seeding and plating. To increase yield, the DNA origami deposition procedure could be altered to increase the percentage that land in an open configuration, or the structures could be attached through multiple chemically specific anchors to better maintain the desired DNA origami shape and decrease aggregation.

Further increases in the yield of metallized structures may also be possible through removing background Au NPs that adsorb to the surface and can lead to undesired metallization. It should be possible to reduce the background particle concentration by adjusting seeding parameters and conditions. Alternatively, chemical attachment of the DNA origami structures to the surface would allow for background reduction by employing more aggressive rinsing techniques. Optimization of these processes and surface attachment will enhance our ability to simultaneously generate very large numbers of successful structures as a basis for nanosystem fabrication and assembly.

CONCLUSION

We have demonstrated a method that uses site-specific attachment of gold nanoparticles and subsequent metallization to fabricate conductive wires from DNA origami templates. An important aspect of the work is the attachment of high densities of Au NPs onto branched DNA origami structures. These closely spaced Au NPs serve effectively as seeds for metallization to create continuous metallized segments or nanowires on origami templates. Continuity was verified via electrical measurements. Additionally, we have shown selective metallization on DNA origami to create geometries with controlled gaps, enabling future fabrication of a wide variety of nanodevices.

MATERIALS AND METHODS

Materials. M13mp18 and streptavidin-coated magnetic beads for DNA scaffold preparation were purchased from New England Biolabs. Staple strands for DNA origami folding and PCR primers were ordered from Operon Biotechnologies (100 μM in TE buffer). Single-stranded DNA thiol was purchased from Operon Biotechnologies with PAGE purification and diluted to 1 mM in water. PCR purification kits were acquired from Qiagen. DNA polymerase and PCR buffers were purchased from Invitrogen or New England Biolabs. 30 kDa Amicon ultra-0.5 mL centrifugal filters were obtained from Millipore. 5 nm Au nanoparticles and mica for AFM imaging were purchased from Ted Pella. BSPP (bis(*p*-sulfonatophenyl)-phenylphosphine dihydrate dipotassium salt) was obtained from Strem Chemicals. (100) n-type silicon wafers were

dx.doi.org/10.1021/jp302316p | J. Phys. Chem. B 2012, 116, 10551−10560

purchased from Silicon Wafer Enterprises, LLC. The silicon monoxide support films on copper TEM grids were purchased from Ted Pella (Product # 01830). The commercial Au plating solution was acquired from Nanoprobes (GoldEnhance EM, Catalog # 2113). Gold(III) chloride trihydrate (≥99.9%) and hydroxylamine (98%) were purchased from Sigma-Aldrich. ZEP-520 electron beam resist and ZED-N50 developer were obtained from Zeon Chemicals. The 1165 Microposit Remover was purchased from MicroChem.

DNA Origami Designs. Branched ("T") shaped DNA origami structures were formed using a 2958 base scaffold, amplified from M13mp18 as previously reported.[33] To enable Au NP attachment, select staple strands from the previously reported design were modified to contain a sequence of 10 adenine nucleotides on the 3′ end. In the initial experiments, 33 staples on one-half of the top section of the "T" structure were modified. For conductivity measurements, the entire top section consisted of modified staple strands (67 in total). For the 'T" structure with a gap, 39 staples were modified. The prototype logic gate structure was folded using M13mp18 for the scaffold with 246 staple strands. 156 of the staple strands contain the extra 10 adenines on the 3′ end for gold nanoparticle attachment.

DNA Origami Folding. Both types of DNA origami structures were folded by heating a mixture of the scaffold and staple strands (2 nM scaffold and 20 nM of each staple strand in 1X TAE-Mg^{2+} buffer) to 95 °C for 3 min and then slowly cooling to 4 °C over 90 min. DNA origami solutions were filtered with 30 kDa Amicon filters, to remove most of the excess staple strands, by centrifuging for 10 min at 13 000 rpm. Samples were rinsed twice with 450−500 μL of either 1× or 10× TAE-Mg^{2+} buffer (10× was used for DNA origami surface seeded samples) by centrifuging for 10 min at 13 000 rpm and recovered by spinning for 3 min at 3500 rpm.

Au NP Preparation. We followed steps similar to those reported previously[16,34] to phosphinate and concentrate the Au NPs with BSPP. More specifically, 1.5 mg of BSPP was added to 5 mL of Au NPs and shaken overnight. 100 mg of NaCl was added, and the solution was centrifuged to pellet the Au NPs. The supernatant was removed, and the Au was resuspended with an aqueous BSPP solution (100 μL, 2.5 mM). Methanol (100 μL) was added, and the solution was centrifuged again to pellet the Au. After removing the supernatant again, the Au was resuspended in aqueous BSPP solution (100 μL, 2.5 mM). The concentration of Au NPs was estimated by comparing the absorption at 520 nm to the absorption of the original gold solution using a Nanodrop 1000 spectrophotometer.

Au NP−DNA Conjugates. Thiolated DNA was used without deprotecting the disulfide bond, as we found the reaction worked either with or without deprotection. Au NPs and thiolated DNA were combined in a 1:200 molar ratio and left to react at room temperature (RT) for at least 19 h. The Au NP DNA conjugates were filtered using 30 kDa Amicon filters to remove unbound thiolated DNA. Samples were rinsed twice during the filtration using 450−500 μL of 0.5× TBE buffer. About 30−35 μL was recovered, with Au NP concentrations around 1−3.5 μM.

Attachment of Au NPs to DNA Origami Structures. For solution attachment of Au NPs to DNA origami structures, DNA origami was combined with the Au NP−DNA conjugates with varying Au NP to DNA origami ratios (of about 1:1, 12:1, 19:1, and 27:1) and cooled from 37 to 20 °C over about 17 min. Then, the solution was deposited onto a mica surface for AFM imaging.

For Au NP surface attachment to DNA origami on SiO_2, DNA origami structures were placed on silicon surfaces using a method reported by Kershner et al.[35] Silicon dioxide surfaces were plasma cleaned (Harrick Plasma Asher; PDC-32G) for 30 s at 18 W to remove contaminants on the surface. Then, 3 μL of filtered DNA origami (2 or 0.67 nM), in 10× TAE/$MgAc_2$ buffer, was allowed to adsorb onto the cleaned surface for 2 h in a humid chamber at RT. The sample was then dipped in a 50% ethanol solution (5 s) and a 90% ethanol solution (1 h). Next, the surface was dried by a stream of filtered air and put back into a humid chamber. Subsequently, 12 μL of seeding solution (Au NP−DNA conjugates diluted in 10× TAE/$MgAc_2$ buffer, 33 nM) was added onto the surface and allowed to seed DNA for 30 min at RT. Afterward, the surface was rinsed in 10× TAE/$MgAc_2$ buffer (5 s), 50% ethanol solution (5 s), and 90% ethanol solution (1 h). Finally, the surface was dried with a stream of filtered air.

Electroless Au Plating. The commercial Au plating solution was prepared according to the manufacturer's instructions. This plating solution was then mixed with an equal volume of $MgCl_2$ solution to yield a final Mg^{2+} concentration of either 2 or 10 mM. The plating was conducted by putting 60 μL of plating solution onto a SiO_2 sample surface at RT. The plating was allowed to proceed for 1, 2, 5, 10, or 20 min. The plating was quenched by rinsing the surface with $MgAc_2$ solution (4 mM Mg^{2+}) for a few seconds, then with water for 2 s, and dried in a stream of filtered air.

Natan's Au plating solution consists of 0.01% (by weight) of $HAuCl_4$ and 0.001% (by weight) of NH_2OH. For this plating process, 60 μL of Natan's Au plating solution was put onto a sample surface (either seeded DNA origami or DNA origami that was plated for 1 min with commercial Au plating solution) and allowed to plate for 2 min. Afterward, the surface was rinsed with a $MgAc_2$ solution (4 mM Mg^{2+}) for a few seconds, then with water for 2 s, and dried with a stream of filtered air.

Conductivity Measurements. Electrode sets were fabricated using standard electron beam lithography methods with ZEP-520 electron beam resist using a Philips XL30 S-FEG scanning electron microscope. Following electron exposure, the resist was developed using ZED-N50 developer. Next, a CHA-600 thermal evaporator (CHA industries) was used to deposit a 5 nm chromium adhesion layer and 40 nm of gold onto the patterned resist. Lift-off of resist was done overnight in the 1165 Microposit remover at RT. Elevated temperatures were avoided, since many origami were removed from the surface when the lift-off temperatures were above 60 °C. Following lift-off, surfaces were rinsed in 2-propanol and dried in a stream of air.

Electrical measurements were performed by using micromanipulator probes to connect two measurement electrodes across a power source. LabVIEW was used both to control the applied voltage and read the current measured from a picoammeter (Ithaco). The voltage was generally ramped from −100 to 100 mV across electrodes. However, to test the stability, up to 1.5 V was applied across some nanowires.

■ ASSOCIATED CONTENT

Ⓢ Supporting Information

AFM images of solution-seeded DNA origami, staple strand sequences, and illustrations of Au NP spacing on DNA origami.

This material is available free of charge via the Internet at http://pubs.acs.org.

AUTHOR INFORMATION

Corresponding Author

*E-mail: atw@byu.edu (A.T.W.); robert_davis@byu.edu (R.C.D.); john_harb@byu.edu (J.N.H.).

Notes

The authors declare no competing financial interest.

ACKNOWLEDGMENTS

The authors gratefully acknowledge funding from the National Science Foundation (CBET-0708347). Gratitude is also expressed to K. Nelson, B. Davis, M. Linford, J. Havican, M. Halbert, W. Yang, and J. Pagaduan of BYU for their help and valuable insights. Gratitude is also expressed to J. Farrer, R. Vanfleet, J. Gardner, and M. Standing for technical support with electron microscopy.

REFERENCES

(1) Li, H. Y.; Carter, J. D.; LaBean, T. H. Nanofabrication by DNA self-assembly. *Mater. Today* **2009**, *12*, 24−32.

(2) Becerril, H. A.; Woolley, A. T. DNA-templated nanofabrication. *Chem. Soc. Rev.* **2009**, *38*, 329−337.

(3) Andersen, E. S.; Dong, M. D.; Nielsen, M. M.; Jahn, K.; Lind-Thomsen, A.; Mamdouh, W.; Gothelf, K. V.; Besenbacher, F.; Kjems, J. DNA origami design of dolphin-shaped structures with flexible tails. *ACS Nano* **2008**, *2*, 1213−1218.

(4) Rothemund, P. W. K. Folding DNA to create nanoscale shapes and patterns. *Nature* **2006**, *440*, 297−302.

(5) Han, D. R.; Pal, S.; Nangreave, J.; Deng, Z. T.; Liu, Y.; Yan, H. DNA Origami with Complex Curvatures in Three-Dimensional Space. *Science* **2011**, *332*, 342−346.

(6) Douglas, S. M.; Dietz, H.; Liedl, T.; Hogberg, B.; Graf, F.; Shih, W. M. Self-assembly of DNA into nanoscale three-dimensional shapes. *Nature* **2009**, *459*, 1154−1154.

(7) Andersen, E. S.; Dong, M.; Nielsen, M. M.; Jahn, K.; Subramani, R.; Mamdouh, W.; Golas, M. M.; Sander, B.; Stark, H.; Oliveira, C. L. P.; Pedersen, J. S.; Birkedal, V.; Besenbacher, F.; Gothelf, K. V.; Kjems, J. Self-assembly of a nanoscale DNA box with a controllable lid. *Nature* **2009**, *459*, 73−76.

(8) Pinheiro, A. V.; Han, D. R.; Shih, W. M.; Yan, H. Challenges and opportunities for structural DNA nanotechnology. *Nat. Nanotechnol.* **2011**, *6*, 763−772.

(9) Torring, T.; Voigt, N. V.; Nangreave, J.; Yan, H.; Gothelf, K. V. DNA origami: a quantum leap for self-assembly of complex structures. *Chem. Soc. Rev.* **2011**, *40*, 5636−5646.

(10) Ke, Y. G.; Lindsay, S.; Chang, Y.; Liu, Y.; Yan, H. Self-assembled water-soluble nucleic acid probe tiles for label-free RNA hybridization assays. *Science* **2008**, *319*, 180−183.

(11) Kuzuya, A.; Kimura, M.; Numajiri, K.; Koshi, N.; Ohnishi, T.; Okada, F.; Komiyama, M. Precisely Programmed and Robust 2D Streptavidin Nanoarrays by Using Periodical Nanometer-Scale Wells Embedded in DNA Origami Assembly. *ChemBioChem* **2009**, *10*, 1811−1815.

(12) Chhabra, R.; Sharma, J.; Ke, Y. G.; Liu, Y.; Rinker, S.; Lindsay, S.; Yan, H. Spatially addressable multiprotein nanoarrays templated by aptamer-tagged DNA nanoarchitectures. *J. Am. Chem. Soc.* **2007**, *129*, 10304−10305.

(13) Rinker, S.; Ke, Y. G.; Liu, Y.; Chhabra, R.; Yan, H. Self-assembled DNA nanostructures for distance-dependent multivalent ligand-protein binding. *Nat. Nanotechnol.* **2008**, *3*, 418−422.

(14) Kuzyk, A.; Laitinen, K. T.; Torma, P. DNA origami as a nanoscale template for protein assembly. *Nanotechnology* **2009**, *20*, 235305.

(15) Maune, H. T.; Han, S. P.; Barish, R. D.; Bockrath, M.; Goddard, W. A.; Rothemund, P. W. K.; Winfree, E. Self-assembly of carbon nanotubes into two-dimensional geometries using DNA origami templates. *Nat. Nanotechnol.* **2010**, *5*, 61−66.

(16) Ding, B. Q.; Deng, Z. T.; Yan, H.; Cabrini, S.; Zuckermann, R. N.; Bokor, J. Gold Nanoparticle Self-Similar Chain Structure Organized by DNA Origami. *J. Am. Chem. Soc.* **2010**, *132*, 3248−3249.

(17) Hung, A. M.; Micheel, C. M.; Bozano, L. D.; Osterbur, L. W.; Wallraff, G. M.; Cha, J. N. Large-area spatially ordered arrays of gold nanoparticles directed by lithographically confined DNA origami. *Nat. Nanotechnol.* **2010**, *5*, 121−126.

(18) Pearson, A. C.; Pound, E.; Woolley, A. T.; Linford, M. R.; Harb, J. N.; Davis, R. C. Chemical Alignment of DNA Origami to Block Copolymer Patterned Arrays of 5 nm Gold Nanoparticles. *Nano Lett.* **2011**, *11*, 1981−1987.

(19) Pal, S.; Deng, Z. T.; Ding, B. Q.; Yan, H.; Liu, Y. DNA-Origami-Directed Self-Assembly of Discrete Silver-Nanoparticle Architectures. *Angew. Chem., Int. Ed.* **2010**, *49*, 2700−2704.

(20) Sharma, J.; Chhabra, R.; Andersen, C. S.; Gothelf, K. V.; Yan, H.; Liu, Y. Toward reliable gold nanoparticle patterning on self-assembled DNA nanoscaffold. *J. Am. Chem. Soc.* **2008**, *130*, 7820.

(21) Zheng, J. W.; Constantinou, P. E.; Micheel, C.; Alivisatos, A. P.; Kiehl, R. A.; Seeman, N. C. Two-dimensional nanoparticle arrays show the organizational power of robust DNA motifs. *Nano Lett.* **2006**, *6*, 1502−1504.

(22) Liddle, J. A.; Gallatin, G. M. Lithography, metrology and nanomanufacturing. *Nanoscale* **2011**, *3*, 2679−2688.

(23) Ozbay, E. Plasmonics: Merging photonics and electronics at nanoscale dimensions. *Science* **2006**, *311*, 189−193.

(24) Tan, S. J.; Campolongo, M. J.; Luo, D.; Cheng, W. L. Building plasmonic nanostructures with DNA. *Nat. Nanotechnol.* **2011**, *6*, 268−276.

(25) Gu, Q.; Cheng, C. D.; Gonela, R.; Suryanarayanan, S.; Anabathula, S.; Dai, K.; Haynie, D. T. DNA nanowire fabrication. *Nanotechnology* **2006**, *17*, R14−R25.

(26) Braun, E.; Eichen, Y.; Sivan, U.; Ben-Yoseph, G. DNA-templated assembly and electrode attachment of a conducting silver wire. *Nature* **1998**, *391*, 775−778.

(27) Richter, J.; Mertig, M.; Pompe, W.; Monch, I.; Schackert, H. K. Construction of highly conductive nanowires on a DNA template. *Appl. Phys. Lett.* **2001**, *78*, 536−538.

(28) Deng, Z. X.; Mao, C. D. DNA-templated fabrication of 1D parallel and 2D crossed metallic nanowire arrays. *Nano Lett.* **2003**, *3*, 1545−1548.

(29) Liu, J. F.; Geng, Y. L.; Pound, E.; Gyawali, S.; Ashton, J. R.; Hickey, J.; Woolley, A. T.; Harb, J. N. Metallization of Branched DNA Origami for Nanoelectronic Circuit Fabrication. *ACS Nano* **2011**, *5*, 2240−2247.

(30) Geng, Y. L.; Liu, J. F.; Pound, E.; Gyawali, S.; Harb, J. N.; Woolley, A. T. Rapid metallization of lambda DNA and DNA origami using a Pd seeding method. *J. Mater. Chem.* **2011**, *21*, 12126−12131.

(31) Pilo-Pais, M.; Goldberg, S.; Samano, E.; LaBean, T. H.; Finkelstein, G. Connecting the Nanodots: Programmable Nanofabrication of Fused Metal Shapes on DNA Templates. *Nano Lett.* **2011**, *11*, 3489−3492.

(32) Schreiber, R.; Kempter, S.; Holler, S.; Schuller, V.; Schiffels, D.; Simmel, S. S.; Nickels, P. C.; Liedl, T. DNA Origami-Templated Growth of Arbitrarily Shaped Metal Nanoparticles. *Small* **2011**, *7*, 1795−1799.

(33) Pound, E.; Ashton, J. R.; Becerril, H. A.; Woolley, A. T. Polymerase Chain Reaction Based Scaffold Preparation for the Production of Thin, Branched DNA Origami Nanostructures of Arbitrary Sizes. *Nano Lett.* **2009**, *9*, 4302−4305.

(34) Loweth, C. J.; Caldwell, W. B.; Peng, X. G.; Alivisatos, A. P.; Schultz, P. G. DNA-based assembly of gold nanocrystals. *Angew. Chem., Int. Ed.* **1999**, *38*, 1808−1812.

(35) Kershner, R. J.; Bozano, L. D.; Micheel, C. M.; Hung, A. M.; Fornof, A. R.; Cha, J. N.; Rettner, C. T.; Bersani, M.; Frommer, J.; Rothemund, P. W. K.; Wallraff, G. M. Placement and orientation of

individual DNA shapes on lithographically patterned surfaces. *Nat. Nanotechnol.* **2009**, *4*, 557−561.
(36) Tinland, B.; Pluen, A.; Sturm, J.; Weill, G. Persistence length of single-stranded DNA. *Macromolecules* **1997**, *30*, 5763−5765.
(37) Satti, A.; Aherne, D.; Fitzmaurice, D. Analysis of scattering of conduction electrons in highly conducting bamboolike DNA-templated gold nanowires. *Chem. Mater.* **2007**, *19*, 1543−1545.
(38) Brown, K. R.; Natan, M. J. Hydroxylamine seeding of colloidal Au nanoparticles in solution and on surfaces. *Langmuir* **1998**, *14*, 726−728.
(39) Aherne, D.; Satti, A.; Fitzmaurice, D. Diameter-dependent evolution of failure current density of highly conducting DNA-templated gold nanowires. *Nanotechnology* **2007**, *18*, 125205.
(40) Park, S.; Chung, S. W.; Mirkin, C. A. Hybrid organic-inorganic, rod-shaped nanoresistors and diodes. *J. Am. Chem. Soc.* **2004**, *126*, 11772−11773.
(41) Ongaro, A.; Griffin, F.; Beeeher, P.; Nagle, L.; Iacopino, D.; Quinn, A.; Redmond, G.; Fitzmaurice, D. DNA-templated assembly of conducting gold nanowires between gold electrodes on a silicon oxide substrate. *Chem. Mater.* **2005**, *17*, 1959−1964.
(42) French, R. H.; Tran, H. V. Immersion Lithography: Photomask and Wafer-Level Materials. *Annu. Rev. Mater. Res.* **2009**, *39*, 93−126.